Enhancement of the Physical and Chemical Stability of Amorphous Drug-Polymer Mixtures via Cryogenic Co-Milling

*Michela Romanini,[1] Marta Lorente,[1] Benjamin Schammé,[2] Laurent Delbreilh,[3] Valérie Dupray,[2] Gérard Coquerel,[2] Josep Lluís Tamarit,[1] Roberto Macovez [1,]**

[1] Grup de Caracterització de Materials, Departament de Física and Barcelona Research Center in Multiscale Science and Engineering, Universitat Politècnica de Catalunya, EEBE, Campus Diagonal-Besòs, Av. Eduard Maristany 10-14, E-08019 Barcelona, Catalonia, Spain.

[2] Laboratoire de Sciences et Méthodes Séparatives SMS-EA3233, Université de Rouen Normandie, F-76821 Mont Saint Aignan, France.

[3] Groupe de Physique des Matériaux, CNRS, INSA Rouen, UNIROUEN, Normandie Université, 76000 Rouen, France

KEYWORDS. Molecular dispersion, cryomilling, polyvinylpyrrolidone, Biclotymol, macromolecular mobility, dielectric spectroscopy

ABSTRACT

Amorphous dispersions of the Biclotymol antiseptic are obtained in polyvinylpyrrolidone (PVP), for different drug loadings, by co-milling at temperature below the glass transition of both components. Characterization of the dispersions by scanning differential calorimetry and temperature-dependent broadband dielectric spectroscopy shows them to be homogeneous amorphous molecular mixtures. A single glass transition with pronounced enthalpy recovery peak is observed, indicative of the formation of a homogeneous glass state characterized by substantial ageing. The polymer has a considerable antiplasticizing effect on the drug, increasing its glass transition temperature (T_g) to well above room temperature. The T_g of the mixture increases linearly with the macromolecular mass fraction. Three (macro)molecular relaxations are identified in the isothermal dielectric spectra of the mixtures. The slowest process corresponds to the cooperative (α relaxation) dynamics of the polymer chains and drug molecules simultaneously, and its relaxation time becomes longer the higher the polymer content. The fastest one is an intramolecular relaxation mode of Biclotymol, and is virtually unaffected by the presence of the polymer. Finally, the intermediate relaxation, which is also observed in pure PVP, is assigned to the motion of the polymer side groups. Its activation barrier increases with increasing drug content, indicative of a direct interaction of the drug with the pyrrolidone moieties, likely via hydrogen bonding to the carbonyl oxygen. Contrary to pure PVP, the mixtures are not hygroscopic. Mechanical amorphization by cryomilling yields thus glassy molecular mixtures at arbitrary drug concentration, with enhanced physical stability against crystallization and enhanced chemical stability against hydrolysis reactions.

Introduction

A large number of drugs and of newly developed compounds with potential pharmacological activity display low solubility in aqueous environments. The low solubility and/or poor temporal dissolution profile hinder the bioavailability and thus the implementation of these drugs in pharmaceutical formulations.[1] One of the ways to improve the dissolution profile of a low-solubility drug is mixing it with an excipient (for example, a polymer) with higher water solubility.[2-5] Formation of binary mixtures with an excipient may also offer the further advantage of enhancing the metastability of the amorphous state[6] of the drug, which is advantageous because the latter state exhibits in general a better dissolution profile than the crystalline drug.[7,8] It has been shown recently[9] that the dissolution profile and apparent solubility of poorly water-soluble drugs can be dramatically enhanced if the drug is mixed with a polymeric excipient such as polyvinylpyrrolidone (PVP), with enhancements of two orders of magnitude with respect to both the crystalline and amorphous states of the pure drug. Dispersion of active pharmaceutical ingredients in polymer matrices can also allow controlled drug release or even targeted delivery.[10,11]

The most versatile way to produce amorphous binary mixtures is the employment of a mechanical method such as roller- or ball-milling.[12] Simultaneous co-milling of pharmaceutical ingredients with a polymer excipient such as PVP has been shown to enhance drug solubility profiles by a factor similar to that obtained with other techniques that yield homogeneous amorphous dispersions, such as spray drying.[13] Mechanical methods offer in principle the advantage that binary mixtures of any two organic materials can be obtained, at any desired relative concentration. Methods based instead on cooling from the melt or on solvent-evaporation from solutions rely instead on the possibility of heating the materials to their melting

point without their decomposition, or on the existence of a suitable, nontoxic common solvent. Their range of applicability and success rate are, moreover, limited by the inherent miscibility limit of the components.[14,15] On the drawbacks side, however, mechanical amorphization does not guarantee that the samples remain amorphous also after the milling process. It may also be wondered if mechanical milling applied to an asymmetric mixture such as a active pharmaceutical principle and a polymeric excipient is always able to produce a truly amorphous mixture at the molecular level, or if instead mechanically induced disorder and mixing are only partial.[16]

In this contribution, we employ differential scanning calorimetry and temperature-dependent dielectric spectroscopy to experimentally investigate the molecular and macromolecular dynamics of amorphous mixtures of PVP with an antiseptic drug, Biclotymol, obtained by a mechanical method. The solid dispersions were achieved by simultaneous cryogenic ball-milling of both components, at polymer mass fractions of 20, 40 and 60%. Some of us have shown recently that cryomilling of Biclotymol with PVP at 4 ºC yielded samples that appeared amorphous in X-ray diffraction experiments, and whose diffraction pattern remained unchanged also after several months of storage at room temperature.[17] We show here that our co-milling procedure results in homogeneous mixing at the molecular level, and study the effect of intermolecular interactions on the glass transition temperature and microscopic dynamics of the amorphous mixtures. We observe the antiplasticizing effect of the polymer excipient on the drug, both on the calorimetric glass transition temperature T_g and on the relaxation time of the associated cooperative structural relaxation (α process). The local relaxation mode of the polymer (γ process), which likely stems from the reorientational motion of the polar pyrrolidone side group,[18] is slightly modified by the presence of the Biclotymol molecules, with an increase

of the activation energy when the drug load increases. On the other hand, we find that the relaxation time of the intramolecular secondary relaxation process[19] of Biclotymol is unaffected by its dispersion in the polymer matrix.

Experimental Methods

Crystalline Biclotymol powder (2,2'-methylenebis(4-chloro-3-methylisopropylphenol, $C_{21}H_{26}Cl_2O_2$, M_w = 381.32 g mol^{-1}) was supplied by Pharmasynthese (Inabata group) and used without further purification. Commercial amorphous Poly-vinylpyrrolidone (PVP, $(C_6H_9NO)_n$, M_w = 40.000 g mol^{-1}) was purchased from Fisher Bioreagents and used as received. Milling experiments were performed in a high energy planetary mill "Pulverisette 7" from Fritsch. Ball milling of PVP and co-milling of PVP with Biclotymol were carried out with two 80 mL milling jars made of zirconium oxide (ZrO_2) containing three balls (Ø = 20 mm) of the same material. A milling temperature of 277 K (4 ^oC) was chosen, not only because it is lower by 16 K than the glass transition temperature of Biclotymol and it was shown in previous studies that amorphous Biclotymol is metastable (during at least few months) at these conditions,[20] but especially because mixed Biclotymol-PVP samples obtained by co-milling at this temperature were found to remain amorphous during at least five months (even when stored at room temperature).[17] An effective 10 h milling experiment (milling periods of 5 min alternated with pauses of the same duration) was conducted with 1 g of material. The vial rotation speed was set to 400 rotations per minute, and the rotation of the solar disk was performed in the opposite direction compared to the vials, with the same absolute value of rotational speed.

The powders obtained by milling were characterized by means of differential scanning calorimetry (DSC), thermogravimetry analysis (TGA) and broadband dielectric spectroscopy

(BDS). Three different binary mixtures were analyzed, with PVP mass fractions of 20, 40, and 60%, respectively. For comparison purposes we also characterized a cryomilled PVP sample. DSC measurements were carried out under N2 atmosphere using a Q100 calorimeter from TA-Instruments. The samples were placed in open pans and characterized between room temperature and 500 K with heating/cooling rates of 10 K min^{-1}. In the case of the cryomilled PVP sample, which was hygroscopic, we also carried out a DSC measurement in a sealed pan to be able to distinguish different contributions from water loss processes. The mass of the samples was determined with a microbalance sensitive to 0.01 mg. TGA scans were acquired while heating the sample in an open vessel under N_2 flow between room temperature (300 K) and 600 K at a rate of 10 K min^{-1}, by means of a Q50 thermobalance from TA-Instruments.

For BDS experiments, the powders obtained by milling were mechanically pressed between stainless steel disks into pellets of submillimeter thickness, and isothermal spectra were acquired in parallel-plate capacitor configuration in the temperature range between 167 and 473 K (with a temperature stability of ± 0.1 K). Measurements were carried out while increasing the temperature to avoid any temperature-induced effect prior to measurement. The spectra were acquired using a Novocontrol Alpha analyzer in the frequency range between 10^{-2} and $5 \cdot 10^{6}$ Hz. Dielectric measurements yield the complex impedance of the sample, from which the complex relative permittivity $\varepsilon^*(\omega) = \varepsilon'(\omega) - i\,\varepsilon''(\omega)$ of the material can be retrieved.

The imaginary permittivity spectra $\varepsilon''(\omega)$ (the so-called "loss spectra") were fitted as the sum of separate spectral components, each representing a different dipolar relaxation dynamics, plus a conductivity background at high temperature. Each relaxation loss was modeled as the imaginary part of a Havriliak-Negami function, whose analytical expression is:[21,22]

(Eq. 1) $\varepsilon_{HN} * (\omega) = \frac{\Delta\varepsilon}{(1+(i\omega\tau_{HN})^c)^d}$.

Here, Δε is the so-called dielectric strength (intensity) of the relaxation process, the exponents *c* and *d* are shape parameters related to the low- and high-frequency tails of the imaginary permittivity (loss) spectrum, and τ_{HN} is a fitting parameter from which the characteristic time τ at which the imaginary part of the permittivity is maximum is obtained as:

(Eq. 2) $\tau = \tau_{HN}\left(\sin\frac{c\pi}{2+2d}\right)^{-1/c}\left(\sin\frac{cd\pi}{2+2d}\right)^{1/c}$.

By fitting the data using Eq. 1 we found that most relaxation losses could be best described as the imaginary part of a Cole-Cole function,[23,24] which is a special case of the Havriliak-Negami function (Eq. 1) with $d = 1$ and $c \neq 1$:

(Eq. 3) $\varepsilon_{CC} * (\omega) = \frac{\Delta\varepsilon}{1+(i\omega\tau)^c}$

While the imaginary part HN is an asymmetric peak, that of the Cole-Cole function is symmetric, and for this model function the parameter τ coincides with the time at which the imaginary permittivity is maximum. Of all the relaxations identified in the loss spectra, only a water-induced relaxation in cryomilled PVP was found to be described by Eq. 1, while all other ones had the symmetric line shape of the imaginary part of the Cole-Cole function.

The loss spectra at high temperature were characterized by a conductivity background which in some cases masked the presence of the relaxation features (especially the cooperative relaxation associated with the glass transition). In such cases, the frequency position of the relaxation process was obtained from the plot of the derivative of the real permittivity versus the logarithm of the frequency:[25]

(Eq. 4) $\varepsilon''_{der}(\omega) = -\frac{\pi}{2}\frac{\partial\varepsilon\prime(\omega)}{\partial ln\omega}$

For relatively broad peaks such as those of primary and secondary relaxations in glass formers, this expression is approximately equal to the ohmic-conduction-free dielectric loss ε”(ω) and thus allows displaying the dielectric loss stemming only from relaxation phenomena, without the

conductivity contribution.[25,26] The spectral position of the maxima in the plot of the derivative of ε'(ω) were taken as initial guesses to perform the fit of the corresponding loss spectrum ε"(ω). Although the Cole-Cole or Havriliak-Negami functions do not account correctly for the spectral lineshape at frequencies far from the loss maximum, it has been shown numerically[27] that these model functions are basically equivalent, under certain conditions, to a time-domain modeling by means of a stretched exponential distribution.

Finally, the contribution of free charge carriers was not a pure conductivity term; their motion was accompanied by polarization effects, visible as an increase in the real part of the permittivity ε'(ω) at low frequency. For this reason, the contribution of free charge carriers to the complex permittivity was modeled with a phenomenological term given by $s_0/[\varepsilon_0(i\omega)^n]$, where n and s_0 are constants.

Results and Discussion.

1. Cryomilled PVP

Figure 1 shows selected isothermal dielectric loss spectra (ε"(*f*), where $f = \omega/2\pi$) of a polymer pellet made with cryomilled PVP. The various panels of Figure 1 display different temperature intervals. The interpretation of the relaxation features visible in the spectra can be carried out in a straightforward way based on the comparison with the dielectric spectroscopy results on amorphous PVP obtained from the melt and on aqueous PVP solutions.[18] Between 150 and 260 K (panel (a)), the polymer spectrum is dominated by a dielectric relaxation (labeled as w_1 in the spectra) which is also observed in aqueous solutions, both at low (1% in weight) and high water concentration, and which is absent in pure PVP.[18] PVP is soluble in water and hygroscopic, so that a certain amount of humidity is unavoidably retained by the samples during storage of the amorphized material and preparation of the pellet for dielectric experiments. The presence of

physisorbed water in the pure PVP samples was confirmed by scanning calorimetry (see Figure 2(a)) and by thermogravimetry analysis (not shown).

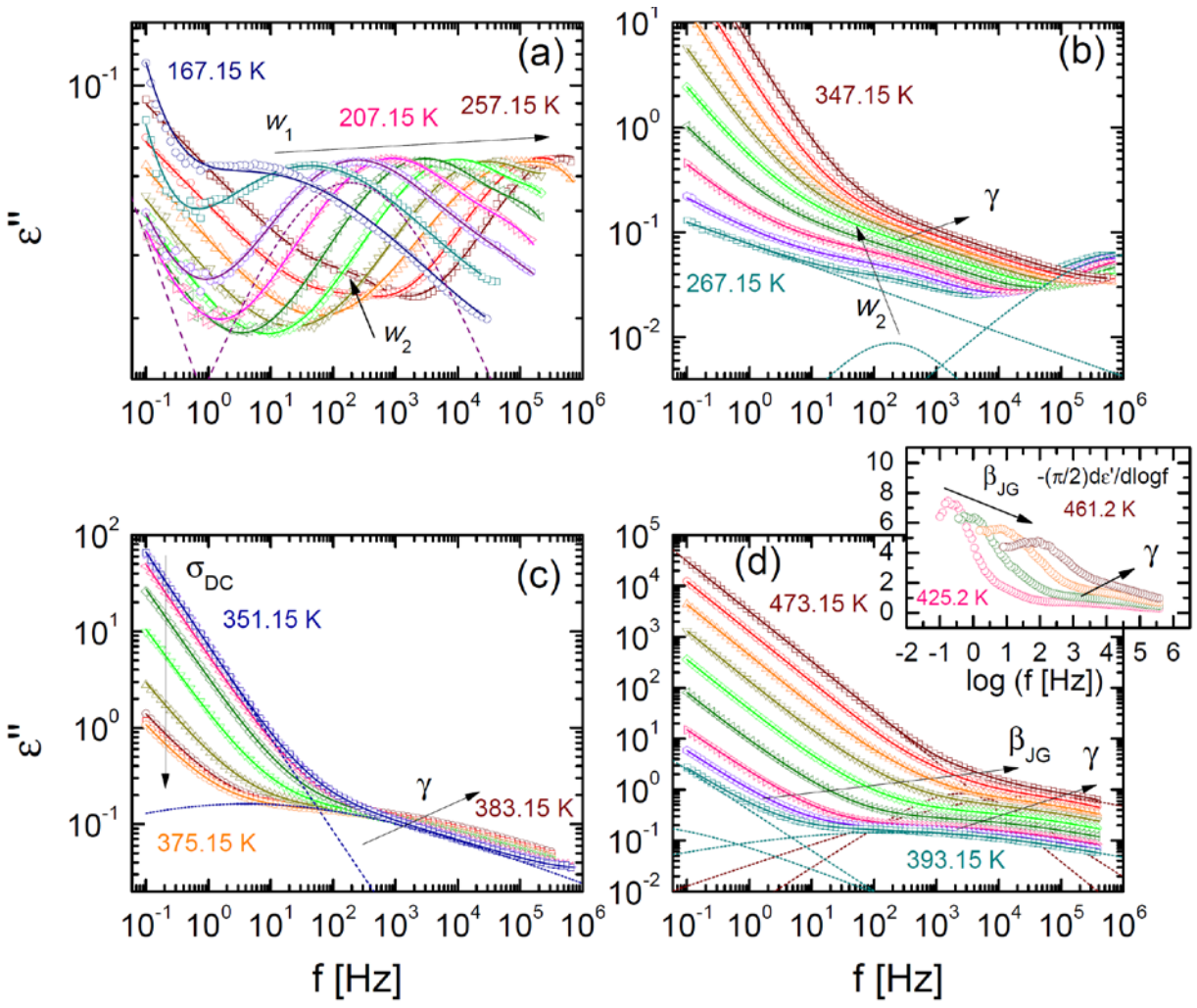

Figure 1. Selected isothermal dielectric loss spectra ε"(*f*) of cryomilled PVP, in different temperature intervals: 167.2-257.2 K, every 10 K (a), where process w_1 is visible; 267.2-347.2 K, every 10 K (b), where process w_2 and γ are observed (together with the low-frequency tail of process w_1); 351.2-383.2 K, every 4 K (c), where the effect of the loss of water is observed as a decrease of the conductivity background, which in turn enhances the visibility of process γ; 393.2-473.2 K, every 10 K (d), where the γ and β_{JG} processes contribute to the spectra. The solid

lines through the data are fits, and dotted lines represent spectral components. Inset to panel (d): logarithmic derivative spectra (eq. 4) of selected high-temperature spectra (425.2-461.2 K, every 12 K) to highlight the presence of both the γ and β_{JG} relaxations.

In the range between 270 and 350 K (Figure 1(b)), another relaxation feature becomes visible, labeled as w_2 in the spectra, while the low-frequency background increases. The w_2 relaxation shows an anomalous temperature behavior, namely, it shifts to lower frequency as the temperature is raised. Water-induced dielectric relaxations with anomalous temperature dependence are typical of hydrated porous or nanostructured materials.[28-34] Such "anomalous" relaxations are generally ascribed to confined water, and the anomalous temperature dependence is rationalized in terms of a reduction of free volume (or equivalently, an increase in the effective pressure) of water molecules (or more in general, hydrogen-bond forming moieties) under confinement.[35-39] Confinement effects are likely to arise in the PVP sample if water molecules are trapped in the inner free volume of the polymer matrix. To the best of our knowledge, the w_2 relaxation was never reported previously in PVP samples. It would appear that its presence is related to the complex porous morphology obtained in the cryomilling process.

Between 350 and 375 K (panel (c)), the typical temperature range where physisorbed water molecules sublimate from hydrated samples, the low frequency background is observed to decrease when the temperature increases. This is a common behavior observed in hydrated organic materials, which most likely reflects the loss of proton conductivity induced by the sublimation of water molecules.[40,41] As the conductivity decreases, a broad relaxation feature becomes visible, labeled as γ, which at lower temperatures was partially buried under the water-induced conductivity contribution. The γ process corresponds to a secondary relaxation dynamics of the polymer.

Finally, panel (d) shows the high-temperature spectra (T > 380 K). While between 370 and 410 K the loss spectrum is characterized by the presence of a single feature (γ relaxation) with roughly constant intensity, above 415 K a significant increase of the loss intensity is observed. This loss enhancement marks the onset of a new relaxation mode of the polymer chains, which is hidden in the low-frequency conductivity background of the spectra of panel (d). To best visualize the presence of two separate relaxations in the high-temperature spectra,[25] in the inset to panel (d) we plot the derivative of the real part of the permittivity (eq. 4) for four representative temperatures. The fact that the lower-frequency feature hidden in the conductivity background is also detected below the calorimetric glass transition temperature of PVP (447 K, see Figure 2(a)) indicates that this relaxation is not the structural α relaxation associated with the glass transition. In fact, a similar relaxation was observed in pure supercooled PVP,**¡Error! Marcador no definido.** where it was assigned to a Johari-Goldstein-like (β_{JG}) relaxation.

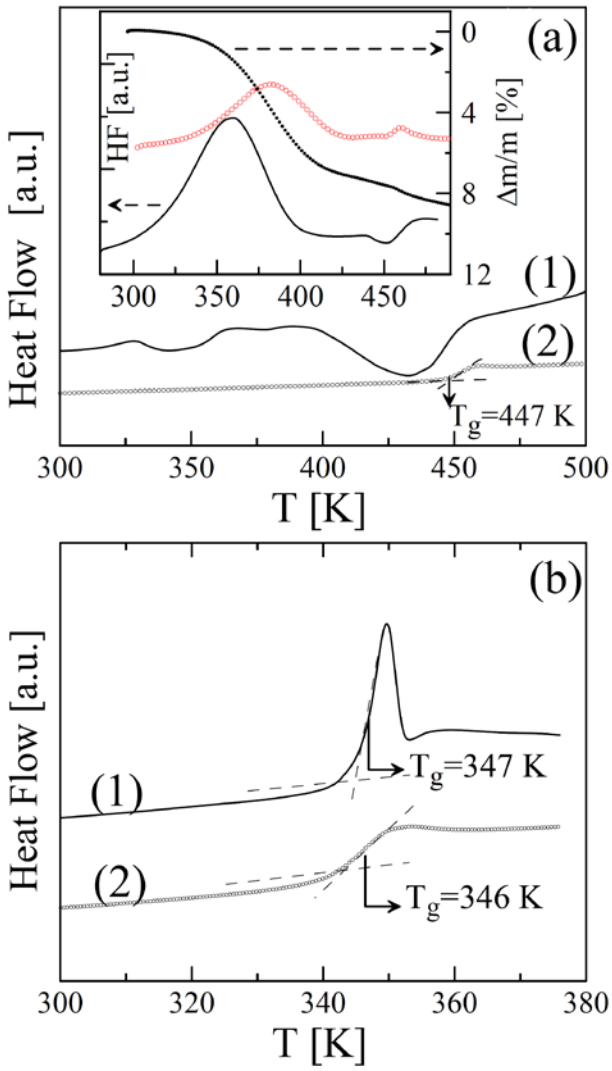

Figure 2. Differential scanning calorimetry thermograms of cryomilled PVP in an initially sealed vessel (a) and of the PVP-Biclotymol mixture with 40% mass content of PVP (b) (endo up). In each panel, the upper curve (continuous line, (1)) corresponds to the first heating scan acquired on the as-stored sample, and the lower curve (open circles, (2)) to the second heating scan measured on the same sample. The glass transition temperatures were determined as indicated. Inset to (a): first-heat DSC (continuous line) and TGA (filled markers) thermograms of cryomilled PVP using an open vessel. The red open markers are the derivative of the TGA trace.

To analyze the temperature dependence of the characteristic relaxation frequency of each loss feature, and allow a better comparison with the data of Cerveny *et al.*,[18] we display in Figure 3 the Arrhenius plot of the relaxation times of the various features identified in the loss spectra of Figure 1. The relaxation times were obtained by fitting each loss peak as the imaginary part of a Cole-Cole function (eq. 3), except for the water-induced w_1 relaxation which was modeled with a Havriliak-Negami function (eq. 1). For the β_{JG} relaxation, since it is not clearly distinguishable in the loss spectra, the fit was performed by setting as initial guess for the relaxation time that obtained from the derivative spectra (eq. 4, see the inset in Figure 1(d)). The presence of two relaxations in this temperature interval (γ and β_{JG} processes) was required to properly model the data and account for the increase of the loss intensity above 415 K; the spectra could not be correctly reproduced with a single spectral component.

For comparison purposes, we show in the plot also the relaxation times of the β_{JG} and γ relaxations of pure supercooled PVP and those of the most prominent water-induced relaxation in a supercooled aqueous solution of PVP with 1% water, after Ref. 18. It may be observed that both the w_1 relaxation and the γ relaxation match approximately the corresponding relaxation times of Ref. 18, which confirms their interpretation in terms respectively of a water-induced relaxation and of a local relaxation mode of the polymer involving the motion of the pyrrolidone side groups. Both relaxations follow the Arrhenius equation:

(Eq. 5) $\tau = \tau_\infty \exp(E_A/k_B T)$.

Here k_B is Boltzmann's constant, τ_∞ is the high-temperature limit of the relaxation time, and E_A is the activation energy for the process. The activation energies are 1.1 and 0.5 eV for the γ and w_1 relaxation, respectively. These values are similar to those reported in Ref. 18. Given that the w_1 relaxation is observed both in the hygroscopic PVP powder and in water solutions of the

polymer, we ascribe this feature to interfacial (surface) water molecules hydrating the polymer chains, but not confined within the polymer bulk. On the basis of its anomalous temperature dependence, we assign instead the w_2 relaxation to water molecules confined in the interstices of the polymer matrix.

The anomalous temperature dependence of water relaxations has been often associated, in recent studies, with the reduction of free volume upon increasing the temperature under confinement. According to a model proposed by Ryabov and coworkers,[36] the increase of temperature in a confined volume has two effects: an increased thermal energy, which speeds up the relaxation dynamics, but also a decrease in the effective free volume available for molecular motions, which is equivalent to an increase in pressure and thus leads to a slowing down of the dynamics. Other theories have been proposed to explain these anomalous water-related relaxations, namely, that they are due to the changes induced in interfacial relaxations upon loss of water. The interfacial relaxation responsible for the anomalous relaxation has been proposed to be a Maxwell-Wagner-Sillar relaxation,[30] or else protonic space-charge polarization.[41] Both mechanisms require the loss of water; however, in the case of cryomilled PVP the anomalous temperature dependence is observed already at temperatures lower than the freezing point of pure water (see Figure 1(b)), which makes it unlikely that it can be an effect of the loss of water molecules. Indeed, the loss of protonic conductivity takes place at significantly higher temperature (Figure 1(c)) than those where the anomalous behavior of the w_2 relaxation is observed. On the other hand, it is likely that our cryomilling process can lead to a mesoporous sample morphology where confinement effects on trapped water molecules may be important. Both water-induced relaxations are significantly slower than the structural relaxation of supercooled bulk-like water, which makes it clear that interfacial water molecules are involved in

both processes;[39] these water-induced relaxations may arise from the relaxation of the molecular dipole moment of strongly bound water molecules, or else from the dynamics of interfacial hydrogen bonds.[41]

It is interesting to note that the calorimetry thermogram of as-stored cryomilled PVP acquired in a sealed vessel (curve labeled (1) in Figure 2(a)) shows the presence of distinct water-induced endothermic peaks, which likely reflect the desorption/evaporation of different types of water molecules (such as physisorbed secondary water, at lower temperature, and confined water, at higher temperature). On the other hand, the DSC and TGA thermograms acquired in open vessels at ambient pressure (see inset to Figure 2(a)) display a very broad water loss in the temperature interval between 320 and 400 K, followed by a mass loss just below the glass transition temperature. The latter may be assigned to the desorption of very-tightly bound water, likely involved in H-bonds with the carbonyl oxygen of the pyrrolidone sidegroups.

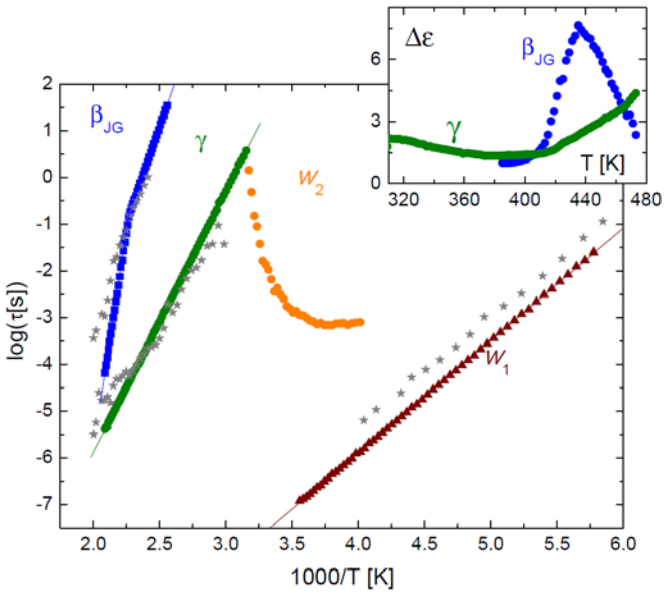

Figure 3. Arrhenius plot of the relaxation times of the four relaxations in cryomilled PVP observed in Figure 1 (processes labeled as w_1, w_2, γ and β_{JG}). For comparison, the relaxation

times of pure PVP obtained by supercooling the melt and PVP aqueous solutions with 1% weight of water are also shown (gray stars, after Ref. 18). Inset: temperature dependence of the dielectric strength Δε of the (polymer-related) β_{JG} and γ relaxations in cryomilled PVP.

The Johari-Goldstein relaxation of glass-formers is closely related with the structural (α) relaxation of these systems, and it usually displays a dynamic crossover at the glass transition temperature (T_g).[42-45] A crossover is observed in both sets of data for the β_{JG} relaxation of PVP (our data and those of Ref. **¡Error! Marcador no definido.**). In our cryomilled PVP sample, the activation energy of the β_{JG} relaxation changes from a high-*T* value of 3.7 eV to a low-*T* value of 1.7 eV. The crossover is observed at 442 K, in rough agreement with the calorimetric T_g (Figure 2(a)), and at virtually the same temperature as the crossover reported in pure supercooled PVP.[18] Small differences in T_g between different PVP samples may be expected due to a different water content and average molecular weight.[18,46]

The inset to Figure 3 displays the dielectric strength (Δε) of the polymer-related relaxations β_{JG} and γ, as a function of temperature. At lower temperatures, the strength of the γ relaxation decreases with increasing temperature, as normally observed in systems with a fixed density of relaxing units (*e.g.*, in the structural relaxation of small-molecule glass formers); the decrease is due to the fact that the effective polarizability of local dipoles is lower the higher the thermal disorder.[47] Starting from ca. 380 K, temperature at which the β_{JG} relaxation enters our experimental frequency window, the strength of the γ process increases with increasing temperature. This is in agreement with the results reported in Ref. 18, and is indicative of the fact that the onset of β_{JG} relaxation has an impact on the local relaxation process. The temperature dependence of the dielectric strength of the β_{JG} relaxation displays a crossover at roughly at the

glass transition temperature, just as the relaxation time does; this effect is in line with the Johari-Goldstein character of this relaxation.[45]

2. PVP-Biclotymol Binary Dispersions

Figure 2(b) shows the DSC thermograms of a representative polymer-drug mixture, namely the one with 40% weight of polymer. In the first heating scan (1) a single glass transition peak with a pronounced enthalpy recovery peak (endothermic overshoot) is visible, indicating that this glassy polymer dispersion has undergone significant ageing during storage.[48] In the subsequent cool-heat cycle (2), a step-like increase in the specific heat was observed at roughly the same temperature as the onset of the glass transition in the first heat up ramp (as-stored sample). Similar results were obtained also at the other polymer concentrations studied: the glass transition temperature was unique, with a significant endothermic overshoot in the first heat-up ramp. The calorimetric glass transition temperature T_g of the samples (as determined from the second heat-up ramp) is reported in Table 1. T_g is found to decrease with increasing drug loading, as it may be expected for a homogeneous mixture where the small-molecule component acts as a polymer plasticizer.

Figure 4 displays the dielectric loss spectra of the same polymer-drug mixture (40% weight of PVP) in two different temperature intervals. The relaxation visible at high frequency in the spectra at lower temperature (panel (a)) matches the spectral position of the secondary relaxation (s_b, where the subscript "*b*" stands for Biclotymol) reported in the pure drug.[19] We observed that the intensity of this feature was higher the larger the Biclotymol content in the mixture. Only this drug-related relaxation was observed in the isothermal spectra at low temperature, while no water-related signal was detected (both the w_1 and w_2 relaxations were absent). Similarly, the

mixture did not exhibit any conductivity anomaly upon warming it through the temperature range of desorption of secondary water. This indicates that no appreciable amount of water is present in the sample, and therefore that the relaxation features observed are exclusively due to the drug and/or to the polymeric excipient. These results show moreover that mixing PVP with Biclotymol effectively reduces the hygroscopic character of the polymer, which is beneficial for the chemical stability of the drug, as it avoids water-induced hydrolysis reactions. We argue that this is due to the direct interaction between the drug molecules and the hydrogen-bond forming group of the macromolecule, namely, the carbonyl group of the pyrrolidone moieties (see also below).

The lowest Biclotymol mass fraction in the mixture is 40%; considering that each Biclotymol molecule has 2 hydroxyl groups, such a high drug content is sufficient to allow most of the carbonyl groups, which in pure PVP are responsible for H-bonding to water molecules, to bind to Biclotymol molecules instead. The loss of hygroscopicity of the mixtures compared to pure PVP indicates that the interaction between the pyrrolidone sidegroups and the drug molecules is stronger than the hydrogen-bond interaction of water to the same group (and to Biclotymol): since water has to compete with Biclotymol to bind to the carbonyl groups, if the interaction with the drug is more favorable than with water, this would effectively remove the adsorption sites for water, rendering the sample less hygroscopic. This interpretation is also consistent with the observed physical stability of the solid-state dispersions, since it is known that amorphous dispersions of drugs in polymers are less prone to crystallize if there is a strong interaction between polymer and drug such as a H-bond interaction.[49,50]

Besides the secondary relaxation, the loss spectra of Figure 4(a) also exhibit a more intense feature, visible in the central portion of the spectra. As will be shown in what follows, this

feature corresponds to the local relaxation mode (γ) of the polymer, which as mentioned is likely related to the reorientational motion of the pyrrolidone side groups. This relaxation is slightly affected by the presence of the Biclotymol molecules, as detailed below.

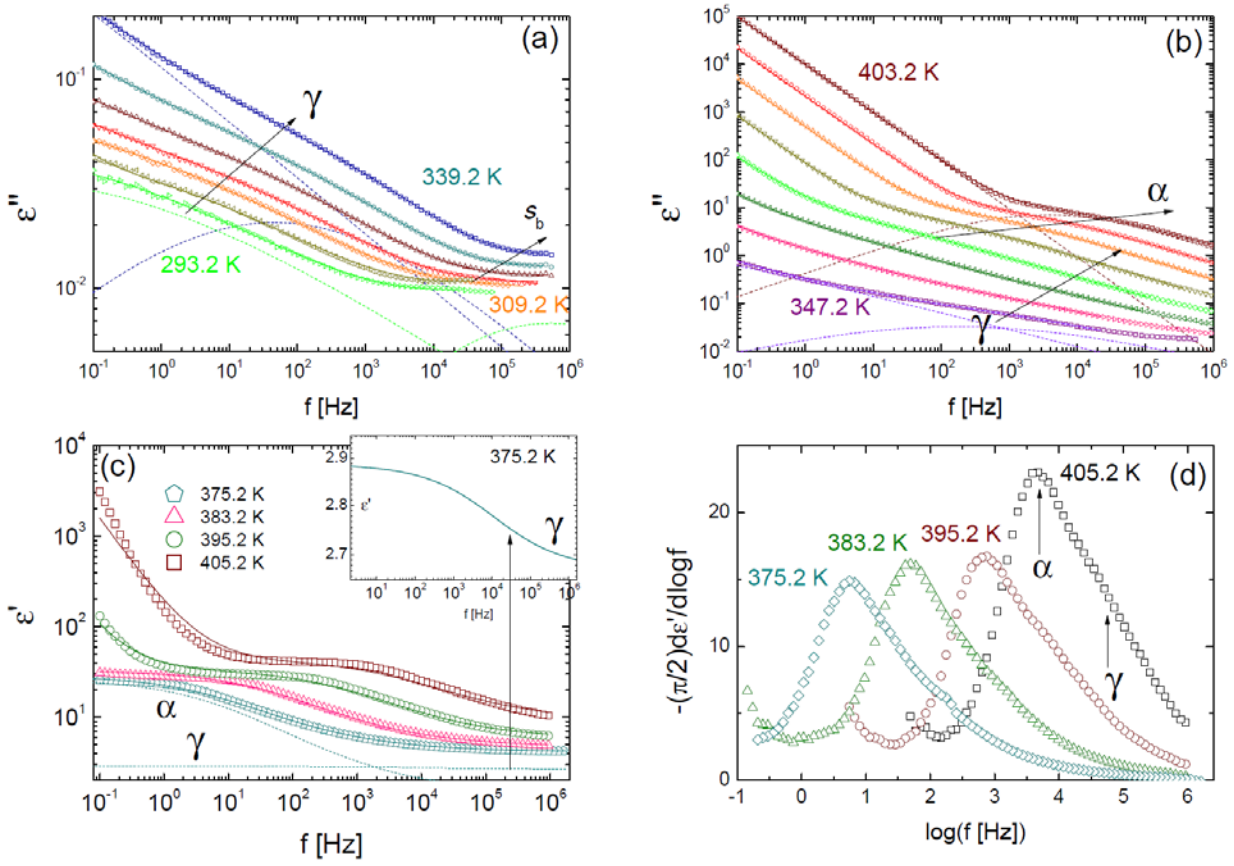

Figure 4. Selected dielectric loss spectra of the cryomilled mixture with 40% weight of PVP, in two different temperature ranges: 293.2-339.2 K (a), and 347.2-403.2 K (b). Markers are experimental data, continuous lines are fits, and dotted lines represent dielectric relaxation or conductivity components. Real permittivity spectra (c) and their derivative as defined in eq. 4 (d) for selected temperatures between 375.2 and 405.2 K. In (c), continuous lines represent the real part of the fit function used to model the imaginary permittivity data, and dotted lines represent

fit components. The inset depicts in detail one of the components, corresponding to the γ relaxation.

At higher temperature (Figure 4(b)) the loss intensity increased significantly due to the onset of a new relaxation feature, which is labeled as α in the spectra. Figure 4(c) shows the real permittivity spectra (ε') at high temperature, for selected temperatures. The other PVP-Biclotymol mixtures studied displayed the same three relaxations, although the secondary relaxation of Biclotymol (s_b) was only barely visible in the sample with 60% mass of PVP. To highlight the presence of two separate relaxations (α, γ) in the loss spectra at higher temperature, in Figure 4(d) we show the derivative plots of the real permittivity (eq. 4) for the same temperatures as in panel (c). The presence of two spectral components, with a predominant α relaxation and a shoulder on the high-frequency flank due to the γ process, can be clearly discerned in this conductivity-free representation. Interestingly, the strength of both relaxations undergoes a sudden increase at about 400 K. A similar sudden increase, even more pronounced than the one observed in Figure 4(d), was also observed in the sample with 20% weight of PVP (not shown). The possible origin of this sudden increase is discussed later.

Figure 5 shows the Arrhenius plot of the relaxation times of all three relaxations observed in the PVP-Biclotymol mixtures. For comparison purposes, the data for the primary (α_b) and secondary (s_b) relaxations of pure amorphous Biclotymol, published in Ref. 19, have also been added to in the graph. It can be observed that the s_b relaxation time is virtually unchanged from one concentration to another, and that it matches that of the pure Biclotymol glass. This, together with the fact that the dielectric strength of this process decreases with decreasing Biclotymol concentration, allows a straightforward interpretation of this relaxation feature in the mixtures as the secondary (non-cooperative) relaxation of the Biclotymol component. Our data furthermore

confirm that the origin of such relaxation is an intramolecular dynamics of the isolated drug molecule, as suggested in Ref. 19, and not a Johari-Goldstein relaxation of the drug.[45]

The other two relaxations in the Arrhenius plot display variations between the samples, which are very significant in the case of the α relaxation. The temperature dependence of the γ relaxation time of the mixtures is simply activated. It can be observed in Figure 5 that the γ relaxation times of both pure PVP and the mixtures appear to converge at room temperature to a value close to Log(τ) = 2. In other words, the temperature at which the relaxation time of this polymer-related dynamics reaches 100 s is the same regardless of the drug loading. The coincidence of the γ relaxation times at low temperatures for all samples including pure PVP indicates that this relaxation dynamics has the same origin in all samples, namely, that they stem from local polymer motions involving the pyrrolidone side groups. The fact that the γ process attains relaxations times longer than 100 s close to the glass transition temperature of Biclotymol, and that therefore the γ relaxation lines cross the primary relaxation line of pure Biclotymol (α_b) near the T_g of the pure drug, is instead purely accidental.

As visible in Figure 5, the γ relaxation times at high temperature are slightly different for different the drug loading. The slope of the γ process in the Arrhenius plot, or equivalently the activation energy E_A, listed in Table 1, increase systematically with increasing drug content. This indicates that the barrier against rotation/tilting of the pyrrolidone moieties increases due to direct interaction of the Biclotymol molecules with the polymer side groups, most likely via hydrogen bonding to the carbonyl oxygen of the pyrrolidone ring. Such direct interaction is responsible for the loss of hygroscopicity of the macromolecules, as the drug molecules cap the hydrogen-bonding group of the PVP moieties. Moreover, it is likely that this relatively strong

drug-excipient interaction contributes substantially to the metastabilization of the amorphous mixtures,[49,50] by preventing the formation of H-bonded homocomponent clusters.

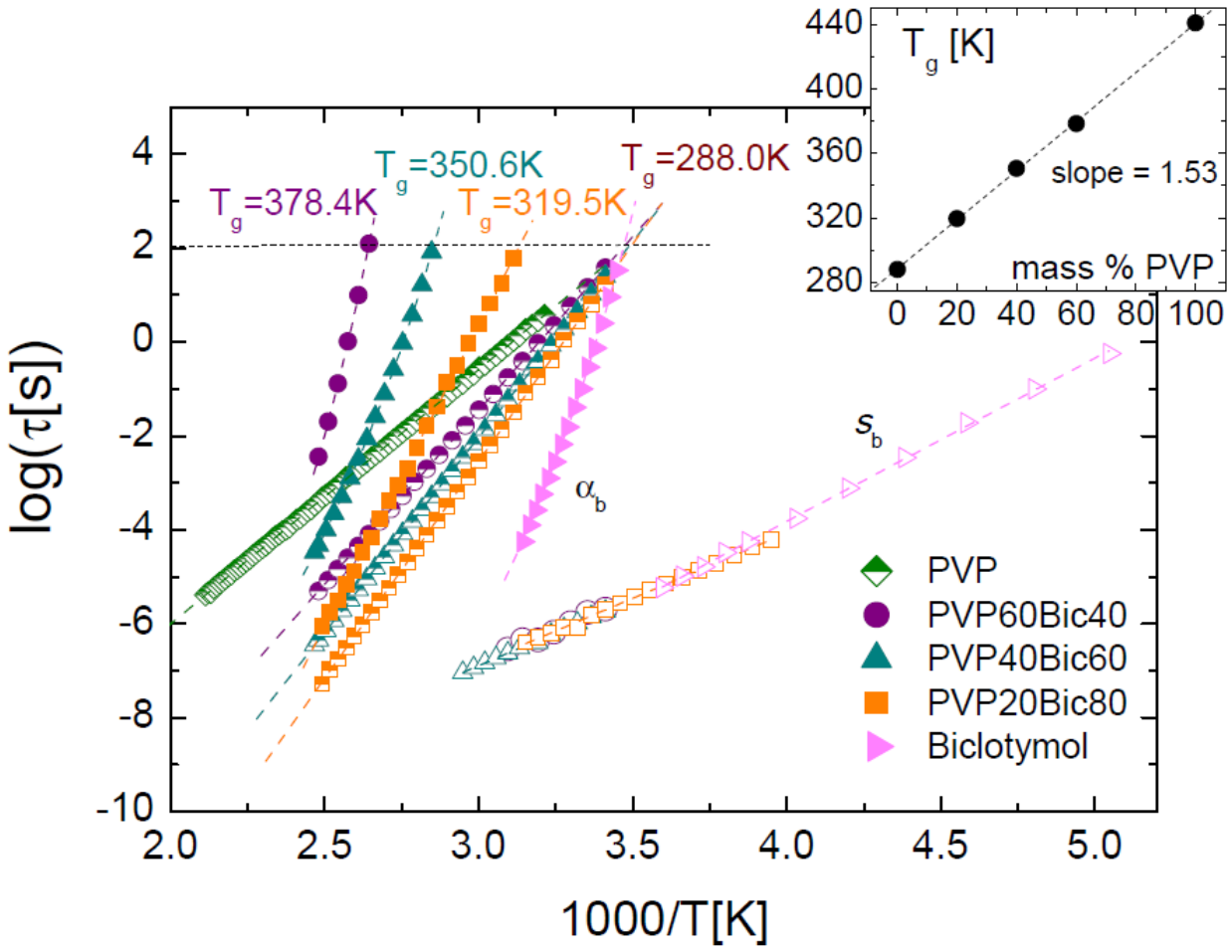

Figure 5. Arrhenius plot of the relaxation times of the Biclotymol intramolecular secondary (empty markers), pyrrolidone side group (semifilled markers), and structural primary (filled markers) relaxation of the PVP-Biclotymol mixtures (20%, 40% and 60% PVP mass fraction). For comparison, the secondary (s_b) and primary (α_b) relaxations of pure Biclotymol are also shown (after Ref. 19). The horizontal dotted line indicates the vitrification time (Log(τ) = 2), while dashed lines are fits with the Arrhenius eq. 5 or with the VFT eq. 6. Inset: plot of the T_g

values extrapolated from dielectric data for binary PVP-Biclotymol samples, as a function of the mass fraction of PVP.

While the γ process follows the Arrhenius law (eq. 5) in all mixtures, the temperature-dependence of the α relaxation time was non-Arrhenius, and was modeled with a Vogel-Fulcher-Tamman (VFT) equation, whose analytical expression is:[51]

(Eq. 6) $\tau_{max} = \tau_\infty \exp[D\, T_{\mathrm{VF}}/(T - T_{\mathrm{VF}})]$.

The prefactor τ_∞, the so-called fragility parameter *D*, and the Vogel-Fulcher temperature T_{VF} are phenomenological parameters. The values obtained by fitting the experimental α relaxation times with eq. 6 are listed in Table 1.

% mass PVP	Log(τ_∞/[ps])	D	T_{VF} [K]	*m*	T_g [K] (BDS)	T_g [K] (DSC) (± 2)	E_A γ relax [eV]
60	–19	15.5	286.7	85	378.4	377	1.48
40	–16.8	18.2	247.1	64	350.6	346	1.66
20	–35.4	955	26.4	41	319.5	321	1.85
0	–19.2	16.2	216.2	85	288.0	292	-

Table 1. VFT parameters of the α relaxation, fragility *m*, and glass transition temperature T_g of PVP-Biclotymol mixtures and Biclotymol. The activation energy (E_A) of the γ relaxation is also listed.

A VFT behavior is typical of cooperative structural relaxations in glass forming systems, and it is obeyed for example by the structural relaxation of pure supercooled Biclotymol.[19] The non-Arrhenius temperature dependence of the process, and the systematic variation of relaxation time and vitrification temperature with polymer weight fraction, allow identifying the high-temperature relaxation process as the structural relaxation of the PVP-Biclotymol mixtures. The

value of the dielectric glass transition temperature T_g for each sample was obtained from the VFT parameters as $T_g = T_{VF}\left(1 + \frac{D}{\mathrm{Ln}(100) - \mathrm{Ln}(\tau_\infty)}\right)$. The dielectric T_g values, listed in Table 1, are in agreement with the calorimetric glass transition temperatures, and both shift to lower values with increasing drug content. As visible in the inset in Figure 5, the dielectric T_g scales with the mass percentage of the polymer in the mixture, increasing by roughly 1.5 K for every percent unit of PVP.

The agreement with the calorimetric T_g and the systematic shift to shorter relaxation times with increasing drug loading confirm that the high temperature relaxation of the mixtures is indeed the structural (α) relaxation. The fact that this relaxation is observed in the mixtures but not in pure PVP might be partially due to the fact that the Biclotymol molecules act as dipolar "markers" that enhance the overall dipole moment of the mixture and thus increase the polarization fluctuations associated with the joint cooperative dynamics. The dielectric strengths Δε of the α relaxations are displayed as a function of temperature in Figure 6(a) for all three mixtures (20, 40, and 60% weight of PVP). The strength of the 40% PVP sample exhibits a continuous increase above T_g (319 K), and then a sudden jump at 400 K, as already noted when discussing Figure 4(c). Similarly, the 20% PVP sample exhibits a sudden increase in strength at 377 K, about 30 K above the glass transition temperature of this mixture.

The increase in strength is opposite to what might be expected from simple thermal arguments, according to which the polarizability of a sample should decrease with increasing temperature due to enhanced thermal fluctuations. We observed similar increases also in pure polymer samples, and their origin is not yet clear. Instead, the relatively sharp changes in dielectric strength were observed only in the mixtures. We consider it unlikely that these changes in

strength reflect a variation of the number of dipolar moieties participating in this dynamic process, as such a variation would have an impact also on the characteristic time of the cooperative motions, which is not observed (Figure 5). Especially in the case of a mixture, the dielectric strength depends not only on the number of cooperatively relaxing units, but also on the relative orientation of the individual neighboring dipoles, which is described by the so-called Kirkwood correlation factor.[47] In a polymer sample, moreover, the strength of the dielectric relaxation depends on whether the monomer dipole is oriented parallel to the chain, or orthogonal to it, or in between. It is likely that the sudden jump in dielectric strength of the α relaxation reflects a different relative orientation of the local dipole moments of the pyrrolidone moieties and Biclotymol molecules, although it cannot be excluded that it is associated with the peculiar character of the amorphous mixtures obtained by the milling procedure. Further independent investigations are needed to clarify this point.

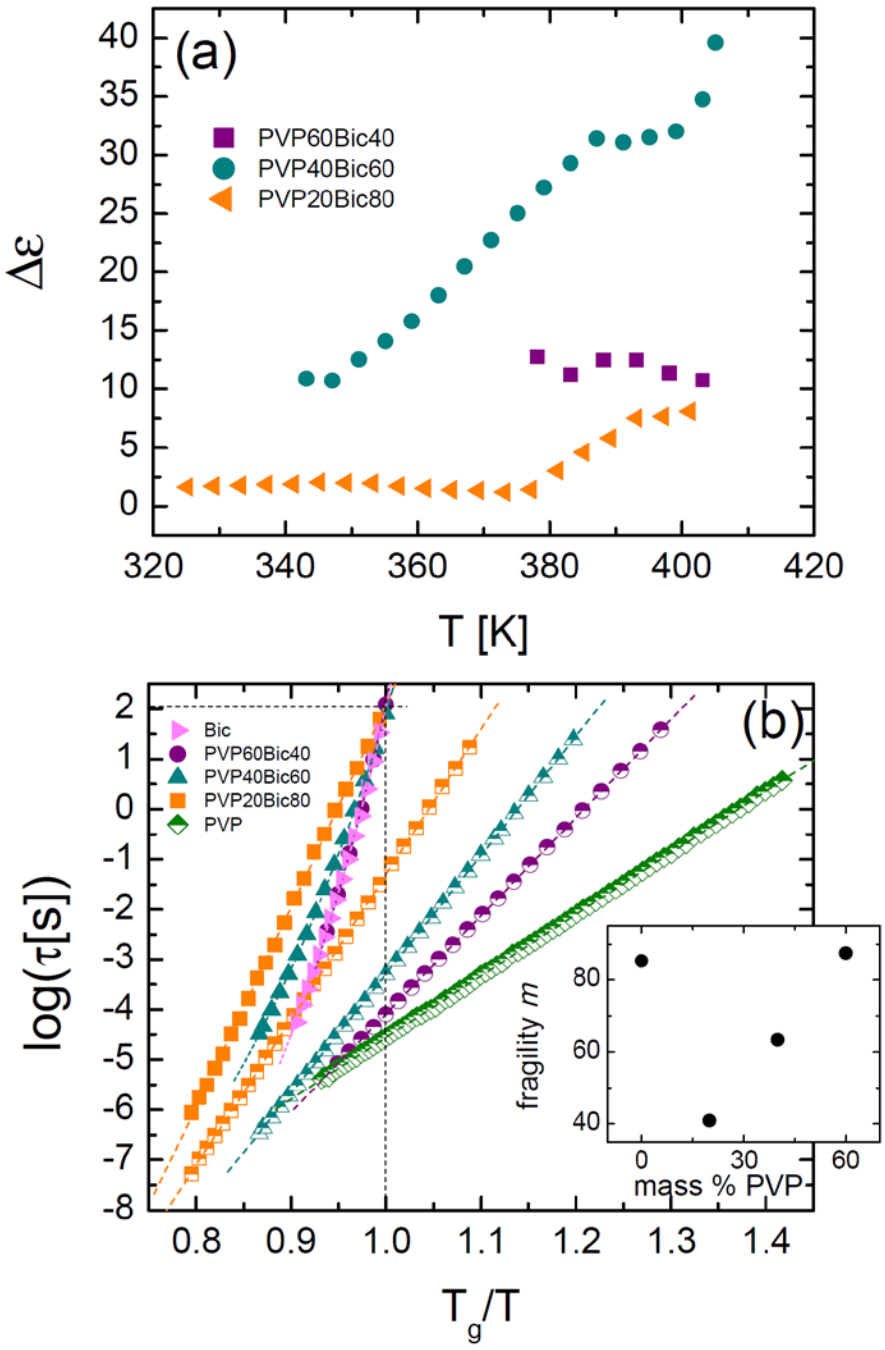

Figure 6. (a) Dielectric strength of the α relaxation of the PVP-Biclotymol mixtures as a function of temperature. (b) Angell plot of the α and γ relaxation times of the mixtures. The data of the γ relaxation of cryomilled PVP and of the α relaxation of pure supercooled Biclotymol are also shown for comparison. Inset: fragility index (*m*) of the mixtures *vs* PVP mass fraction.

The observation of a cooperative dynamics whose relaxation time scales with the amount of Biclotymol is clear evidence that our cryogenic milling procedure yields truly molecular mixtures, with the drug molecules in direct contact with the polymer chains. The results of our analysis also rule out a possible presence of an amorphous pure Biclotymol fraction. It is worth mentioning that no crystallization of the Biclotymol component is observed in the experimental runs, despite the fact that the samples were heated up to 455 K, that is, more than 100 K higher than the onset of the recrystallization process of pure supercooled Biclotymol.[19]

While the structural relaxation time and thus the viscosity of the sample decrease significantly with increasing Biclotymol content, the γ relaxation time appears to be only slightly affected by this change in the macroscopic properties of the mixture and by the enhancement of the cooperative segmental motions (see Figure 5). This entails that the frequency separation between the α and γ decreases with increasing drug loading. To best visualize this, Figure 6(b) shows the Angell plot (Log(τ) *vs* T_g/T) of both polymer-related relaxations for all studies samples (for the case of pure PVP, the definition of the normalized temperature scale was done taking the calorimetric glass transition temperature of 447 K). The γ relaxation does not scale with T_g, which confirms that it does not have a Johari-Goldstein character, since Johari-Goldstein relaxations maintain a fixed frequency separation with respect to the cooperative α relaxation.[45,52]

The most important parameter of the α relaxation in the Angell plot is the so-called kinetic fragility,[53,54] defined as the slope at $T_g/T = 1$. In the case of structural relaxations following a VFT behavior, it can be computed as $m = \frac{D}{\mathrm{Ln}(10)} \frac{T_{VF}/T_g}{\left(1-T_{VF}/T_g\right)^2}$. The fragility is observed in the main panel and inset of Figure 6(b) to be a function of the composition of the mixtures, in

particular, it is lower the lower the PVP mass fraction. The obtained fragility values are listed in Table I. The mixture with 20% mass fraction of PVP (80% mass fraction of Biclotymol) behaves as a relatively strong glass former, which is surprising given that pure Biclotymol has a fragility value of about 85 ± 10.

Concerning again the γ relaxation, it may be seen in the Angell plot that the relaxation time of the local relaxation mode of the polymer at T_g (that is, for a fixed value of the viscosity) is not constant, but it is instead lower the higher the drug loading. The same is true also at temperatures other than T_g: for a fixed value of the normalized temperature T/T_g, the γ relaxation becomes slower the higher the drug content. The results of Figure 5 and Figure 6(b) can be rationalized as follows. The presence of the Biclotymol molecules, whose linear dimensions are small compared to the gyration radius of the polymer, increases the free volume available for cooperative segmental motions of the polymer, resulting in a plasticizing effect of the drug on the α dynamics. On the other hand, the direct interaction of the Biclotymol molecules with the polymer side groups increases the "effective mass" of the pyrrolidone moieties and enhances their steric interactions, slowing down their rotation/tilting motion with respect to the chain and resulting in an effective relative antiplasticizing effect on the γ dynamics. The side group relaxation cannot obviously be independent of the chain dynamics; the rough coincidence of γ relaxation times between the samples at low temperature would then stem from the compensation of plasticizing and antiplasticizing effects.

Our results show that obtaining binary mixtures is not only a valuable tool to metastabilize the thermodynamically unstable glassy phases of the pure components,[55,56] but that it also allows to unambiguously identify secondary relaxations, a task that is not always trivial.[57,58] They further

show that cryogenic co-milling leads to the establishment of relatively strong H-bond interactions that boost both the physical stability of the mixed samples, by preventing the nucleation of separate phases of the two components, and the chemical stability during storage, by preventing the capture of water vapor by the hydrophilic water-soluble polymer carrier. It is possible that the formation of stable H-bonds is at least partially due to the application of the milling method at temperatures below the glass transition of either component, where cooperative motions are quenched; this might induce the formation of more stable local interactions by bringing the two components close together by mechanical (pressure-like) forces, at a temperature where the system has not enough thermal energy to overcome the hydrogen bond network to promote a cooperative structural relaxation.

Conclusion.

We have employed differential scanning calorimetry and broadband dielectric spectroscopy to characterize cryomilled polyvinylpirrolidone (PVP) and amorphous solid dispersions of the Biclotymol antiseptic in PVP obtained by cryogenic co-milling. Cryomilling of PVP results in an amorphous matrix with similar glass transition temperature than supercooled PVP. The as-stored PVP sample is observed to contain a minority fraction of water; the dielectric spectra exhibit four relaxation processes, two of which are due to water, and two to the polymer. On the contrary, no evidence of water is found in the binary drug-polymer mixtures. The glass transition temperature of the dispersion scales linearly with the polymer content, and no crystallization of the drug is also observed at high temperature, contrary to the case of pure Biclotymol which crystallizes at temperatures just above its glass transition temperature. Hence, mixing the drug with PVP boosts the metastability of the amorphous formulation. The dielectric spectra of the mixtures show the existence of three dielectric relaxations, one of which is the cooperative structural relaxation of

the mixture, and the other two correspond to the local relaxation mode of each component, respectively. The local relaxation mode of the polymer, associated with a reorientational motion of the pyrrolidone sidegroup, is affected by the presence of the drug, which not only acts as a "marker" to enhance the visibility of reorientational motions, but also increases the energy barrier for these local reorientational processes.

Our work shows that cryogenic ball milling is able to produce a molecular mixture also in the case of an asymmetric binary system composed of a small-molecule drug and a macromolecular excipient. The local interactions between drug and polymer effectively enhance the physical and chemical stability of the mechanically obtained mixtures.

AUTHOR INFORMATION

Corresponding Author

* Author to whom correspondence should be addressed. Electronic mail: roberto.macovez@upc.edu.

Author Contributions

The manuscript was written through contributions of all authors. All authors have given approval to the final version of the manuscript.

ACKNOWLEDGMENT

This work has been partially supported by the Spanish Ministry of Economy and Competitiveness MINECO through project FIS2017-82625-P and by the Generalitat de Catalunya under project 2017SGR-42.

ABBREVIATIONS

PVP, polyvinylpyrrolidone; VFT, Vogel-Fulcher-Tamman.

REFERENCES

1. Williams, H. D.; Trevaskis, N. L.; Charman, S. A.; Shanker, R. M.; Charman, W. N.; Pouton, C. W.; Porter, C. J. H. Strategies to Address Low Drug Solubility in Discovery and Development. *Pharmacol. Rev.* **2013**, *65*, 315-499

2. Murdande, S.B.; Di Nunzio, J.C.; Miller, D. A.; Yang, W.; McGinity, J. W.; Williams, R. O. III. Amorphous Compositions Using Concentration Enhancing Polymers for Improved Bioavailability of Itraconazole. *Mol. Pharm.* **2008**, *5*, 968–980

3. Marsac, P.; Shamblin, S.; Taylor, L. Theoretical and Practical Approaches for Prediction of Drug-Polymer Miscibility and Solubility. *Pharm. Res.* **2006**, *23*, 2417-2426

4. Pikal, M. J.; Shanker, R. M.; Bogner, R. H. Solubility Advantage of Amorphous Pharmaceuticals: I. A Thermodynamic Analysis. *J. Pharm. Sci.* **2010**, *99*, 1254-1264

5. Kaneniwa, N.; Ikekava, A. Solubilization of Water-Insoluble Organic Powders by Ball-Milling in the Presence of Polyvinylpyrrolidone, *Chem. Pharm. Bull.* **1975**, *23*, 2973–2986

6. Ruiz, G. N.; Romanini, M.; Barrio, M.; Tamarit, J. Ll.; Pardo, L. C.; Macovez, R. Relaxation Dynamics vs Crystallization Kinetics in the Amorphous State: The Case of Stiripentol. *Mol. Pharm.* **2017**, *14*, 3636–3643

7. Gupta, P.; Chawla, G.; Bansal, A.P. Physical Stability and Solubility Advantage from Amorphous Celecoxib: the Role of Thermodynamic Quantities and Molecular Mobility. *Mol. Pharm.* **2004**, *1*, 406–413

8. Craig, D.Q.M.; Royall, P.G.; Kett, V.L.; Hopton, M.L. The Relevance of the Amorphous State to Pharmaceutical Dosage Forms: Glassy Drugs and Freeze Dried Systems. *Int. J. Pharm.* **1999**, *179*, 179–207

9. Szczurek, J.; Rams-Baron, M.; Knapik-Kowalczuk, J.; Antosik, A.; Szafraniec, J.; Jamróz, W.; Dulski, M.; Jachowicz, R.; Paluch, M. Molecular Dynamics, Recrystallization Behavior, and Water Solubility of the Amorphous Anticancer Agent Bicalutamide and Its Polyvinylpyrrolidone Mixtures. *Mol. Pharm.* **2017**, *14*, 1071−1081

10. Liechty, W. B.; Kryscio, D. R.; Slaughter, B. V.; Peppas, N. A. Polymers for Drug Delivery Systems. *Annu. Rev. Chem. Biomol. Eng.* **2010**, *1*, 149–173

11. Ulbrich, K.; Holá, K.; Šubr, V.; Bakandritsos, A.; Tuček, J.; Zbořil, R. Targeted Drug Delivery with Polymers and Magnetic Nanoparticles: Covalent and Noncovalent Approaches, Release Control, and Clinical Studies. *Chem. Rev.* **2016**, *116*, 5338–5431

12. Z. H. Loh, A. K. Samanta, P. W. Sia Heng. Overview of milling techniques for improving the solubility of poorly water-soluble drugs. *Asian J. Pharm. Sci.* **2015**, *10*, 255-274

13. Caron, V.; Tajber, L.; Corrigan, O. I.; Healy, A. M. A Comparison of Spray Drying and Milling in the Production of Amorphous Dispersions of

Sulfathiazole/Polyvinylpyrrolidone and Sulfadimidine/Polyvinylpyrrolidone. *Mol. Pharm.* **2011**, *8*, 532–542

14. Patil, H.; Tiwari, R. V.; Repka, M. A. Hot-melt extrusion: from theory to application in pharmaceutical formulation. *AAPS Pharm. Sci. Tech.* **2016**, *17*, 20-42

15. Vasconcelos, T.; Marques S.; das Neves, J.; Sarmento, B. Amorphous solid dispersions: Rational selection of a manufacturing process. *Adv. Drug Deliv. Rev.* **2016**, *100*, 85-101

16. Descamps, M.; Willart, J. F. Perspectives on the amorphisation/milling relationship in pharmaceutical materials. *Adv. Drug Deliv. Rev.* **2016**, *100*, 51-66

17. Schammé, B.; Couvrat, N.; Malpeli, P.; Dudognon, E.; Delbreilh, L.; Dupray, V.; Dargent, E.; Coquerel, G. Transformation of an Active Pharmaceutical Ingredient upon High-Energy Milling: A Process-Induced Disorder in Biclotymol. *Int. J. Pharm.* **2016**, *499*, 67-73

18. Cerveny, S.; Alegría, A.; Colmenero, J. Broadband Dielectric Investigation on Poly(Vinyl Pyrrolidone) and its Water Mixtures. *J. Chem. Phys.* **2008**, *128*, 044901

19. Tripathi, P.; Romanini, M.; Tamarit, J. Ll.; Macovez, R. Collective Relaxation Dynamics and Crystallization Kinetics of the Amorphous Biclotymol Antiseptic. *Int. J. Pharm.* **2015**, *495*, 420–427

20. Schammé, B., Couvrat, N., Malpeli, P., Delbreilh, L., Dupray, V., Dargent, E., Coquerel, G. Crystallization Kinetics and Molecular Mobility of an Amorphous Active Pharmaceutical Ingredient: a Case Study with Biclotymol. *Int. J. Pharm.* **2015**, *490*, 248-257

21. Havriliak S.; Negami, S. A Complex Plane Analysis of α-Dispersions in Some Polymer Systems. *J. Polym. Sci.-Pt. C* **1966**, *16*, 99−117

22. Havriliak S.; Negami, S. A Complex Plane Representation of Dielectric and Mechanical Relaxation Processes in Some Polymers. *Polymer* **1967**, *8*, 161−210

23. Cole, K.S.; Cole, R.H. Dispersion and Absorption in Dielectrics - I Alternating Current Characteristics. *J. Chem. Phys.* **1941**, *9*, 341–352

24. Cole, K.S.; Cole, R.H. Dispersion and Absorption in Dielectrics - II Direct Current Characteristics. *J. Chem. Phys.* **1942**, *10*, 98–105

25. Steeman, P.A.M.; van Turnhout, J. Fine Structure in the Parameters of Dielectric and Viscoelastic Relaxations. *Macromolecules* **1994**, *27*, 5421-5427

26. Wübbenhorst, M.; van Turnhout, J. Analysis of Complex Dielectric Spectra. I. One-Dimensional Derivative Techniques and Three-Dimensional Modeling. *J. Non-Cryst. Solids* **2002**, *305*, 40–49

27. Alvarez, F.; Alegra A.; Colmenero, J. Relationship between the Time-Domain Kohlrausch-Williams-Watts and Frequency-Domain Havriliak-Negami Relaxation Functions. *Phys. Rev. B* **1991**, *44*, 7306

28. Haspel, H.; Bugris,V.; Kukovecz, Á. Water Sorption Induced Dielectric Changes in Titanate Nanowires. *J. Phys. Chem. C* **2013**, *117*, 16686–16697

29. Jansson, H.; Swenson, J. Dynamics of Water in Molecular Sieves by Dielectric Spectroscopy. *Eur. Phys. J.* **2003**, *E12*, S51

30. Sjöström, J.; Swenson, J.; Bergman, R.; Kittaka, S. Investigating Hydration Dependence of Dynamics of Confined Water: Monolayer, Hydration Water and Maxwell–Wagner Processes. *J. Chem. Phys.* **2008**, *128*, 154503-154508

31. Frunza, L.; Kosslick, H.; Frunza, S.; Schönhals, A. Unusual Relaxation Behavior of Water Inside the Sodalite Cages of Faujasite–Type Molecular Sieves. *J. Phys. Chem. B* **2002**, *106*, 9191–9194

32. Jastrzebska, M.; Kocot, A.; Vij, J.K.; Zalewska-Rejdak, J.; Witecki, T. Dielectric Studies on Charge Hopping in Melanin Polymer. *J. Mol. Struct.* **2002**, *606*, 205-210

33. Le Caër, S.; Lima, M.; Gosset, D.; Simeone, D.; Bergaya, F.; Pommeret, S.; Renault, J.-Ph.; Righini R. Dynamics of Water Confined in Clay Minerals. *J. Phys. Chem. C* **2012**, *116*, 12916−12925

34. Cerveny, S.; Barroso-Bujans, F.; Alegrıa, A.; Colmenero J. Dynamics of Water Intercalated in Graphite Oxide. *J. Phys. Chem. C* **2010**, *114*, 2604–2612

35. Ryabov, Y.; Gutina, A.; Arkhipov, V.; Feldman Y. Dielectric Relaxation of Water Absorbed in Porous Glass. *J. Phys. Chem. B* **2001**, *105*, 1845-1850

36. Ryabov, Y. E.; Puzenko, A.; Feldman, Y. Nonmonotonic Relaxation Kinetics of Confined Systems. *Phys. Rev. B* **2004**, *69*, 014204

37. Frunza, L.; Kosslick, H.; Pitsch, I.; Frunza, S.; Schönhals, A. Rotational Fluctuations of Water Inside the Nanopores of SBA–Type Molecular Sieves. *J. Phys. Chem. B* **2005**, *109*, 9154–9159

38. Grzybowska, K.; Grzybowski, A.; Paluch, M. Role of Defects in the Nonmonotonic Behavior of Secondary Relaxation of Polypropylene Glycols. *J. Chem. Phys.* **2008**, *128*, 134904

39. Macovez, R.; Mitsari, E.; Zachariah M.; Romanini, M.; Zygouri, P.; Gournis D.; Tamarit, J. Ll. Ultraslow Dynamics of Water in Organic Molecular Solids. *J. Phys. Chem. C* **2014**, *118*, 4941–4950

40. Zachariah, M.; Mitsari, E.; Romanini, M.; Zygouri, P.; Gournis, D.; Barrio, M.; et al. Water-Triggered Conduction Mediated by Proton Exchange in a Hygroscopic Fulleride and its Hydrate. *J. Phys. Chem. C* **2015**, *119*, 685–694

41. Mitsari, E.; Romanini, M.; Barrio, M.; Tamarit, J. Ll.; Macovez, R. Protonic Surface Conductivity and Proton Space-Charge Relaxation in Hydrated Fullerol. *J. Phys. Chem. C* **2017**, *121*, 4873–4881

42. Fujima, T.; Frusawa, H.; Ito, K. Merging of α and Slow β Relaxation in Supercooled Liquids. *Phys. Rev. E* **2002**, *66*, 031503

43. Paluch, M.; Roland, C. M.; Pawlus, S.; Zioło, J.; Ngai K. L. Does the Arrhenius Temperature Dependence of the Johari-Goldstein Relaxation Persist above Tg? *Phys. Rev. Lett.* **2003**, *91*, 115701

44. Kessairi, K.; Capaccioli, S.; Prevosto, D.; Lucchesi, M.; Sharifi, S.; Rolla, P. A. Interdependence of Primary and Johari-Goldstein Secondary Relaxations in Glass-Forming Systems. *J. Phys. Chem. B* **2008**, *112*, 4470-4473

45. Ngai, K. L.; Paluch, M. Classification of secondary relaxation in glass-formers based on dynamic properties. *J. Chem. Phys.* **2004**, *120*, 857-873

46. Buera, M. D.; Levi, G.; Karel, M. Glass Transition in Poly(Vinyl Pyrrolidone): Effect of Molecular Weight and Diluents. *Biotechnol. Prog.* **1992**, *8*, 144-148

47. Kremer, F.; Schönhals, A. Broadband Dielectric Spectroscopy. Springer: Berlin, 2003

48. Boucher, V. M.; Cangialosi, D.; Alegría, A.; Colmenero, J. Enthalpy Recovery of Glassy Polymers: Dramatic Deviations from the Extrapolated Liquidlike Behavior. *Macromolecules* **2011**, *44*, 8333–8342

49. Mistry, P.; Mohapatra, S.; Gopinath, T.; Vogt, F, G.; Suryanarayanan, R. Role of the Strength of Drug–Polymer Interactions on the Molecular Mobility and Crystallization Inhibition in Ketoconazole Solid Dispersions. *Mol. Pharm.* **2015**, *12*, 3339–3350

50. Kothari, K.; Ragoonanan, V.; Suryanarayanan, R. The Role of Drug−Polymer Hydrogen Bonding Interactions on the Molecular Mobility and Physical Stability of Nifedipine Solid Dispersions. *Mol. Pharm.* **2015**, *12*, 162–170

51. Angell, C. A. Structural Instability and Relaxation in Liquid and Glassy Phases near the Fragile Liquid Limit. *J. Non-Cryst. Solids* **1988**, *102*, 205–221

52. Romanini, M.; Barrio, M.; Macovez, R.; María D. Ruiz-Martin, M. D.; Capaccioli, S.; Tamarit, J. Ll. Thermodynamic Scaling of the Dynamics of a Strongly Hydrogen-Bonded Glass-Former. *Sci. Rep.* **2017**, *7*, 1346

53. Angell, C. A. Spectroscopy Simulation and Scattering, and the Medium Range Order Problem in Glass. *J. Non-Cryst. Solids* **1985**, *73*, 1–17

54. Böhmer, R.; Ngai, K.L.; Angell, C.; Plazek, D. Nonexponential Relaxations in Strong and Fragile Glass Formers. *J. Chem. Phys.* **1993**, *99*, 4201−4209

55. Bauer, Th.; Köhler, M.; Lunkenheimer, P.; Loidl, A.; Angell, C. A. Relaxation Dynamics and Ionic Conductivity in a Fragile Plastic Crystal. *J. Chem. Phys.* **2010**, 133, 144509

56. Zachariah, M.; Romanini, M.; Tripathi, P.; Barrio, M.; Tamarit, J.L.; Macovez, R. Self-Diffusion, Phase Behavior, and Li+ Ion Conduction in Succinonitrile-Based Plastic Cocrystals. *J. Phys. Chem. C* **2015**, 119, 27298–27306

57. Romanini, M.; Barrio, M.; Capaccioli, S.; Macovez, R.; Ruiz-Martin, M. D.; Tamarit, J. Ll. Double Primary Relaxation in a Highly Anisotropic Orientational Glass-Former with Low-Dimensional Disorder. *J. Phys. Chem. C* **2016**, *120*, 10614-10621

58. Romanini, M.; Mitsari, E.; Tripathi, P.; Serra, P.; Zuriaga, M.; Tamarit, J. Ll.; Macovez, R. Simultaneous Orientational and Conformational Molecular Dynamics in Solid 1,1,2-Trichloroethane. *J. Phys. Chem. C* **2018**, *122*, 5774-5783

for Table of Contents use only

Enhancement of the Physical and Chemical Stability of Amorphous Drug-Polymer Mixtures via Cryogenic Co-Milling

Michela Romanini, Marta Lorente, Benjamin Schammé, Laurent Delbreilh, Valérie Dupray, Gérard Coquerel, Josep Lluís Tamarit, and Roberto Macovez

TOC GRAPHICS